Mon. Not. R. Astron. Soc. **341,** 937–940 (2003)

A measurement of H_0 from Ryle Telescope, *ASCA* and *ROSAT* observations of Abell 773

Richard Saunders,[1⋆] Rüdiger Kneissl,[1] Keith Grainge,[1] William F. Grainger,[1] Michael E. Jones,[1] Alessia Maggi,[2] Rhiju Das,[1†] Alastair C. Edge,[3] Anthony N. Lasenby,[1] G. G. Pooley,[1] Shigeru J. Miyoshi,[4] Taisuke Tsuruta,[4] Koujun Yamashita,[5] Yuzuru Tawara,[5] Akihiro Furuzawa,[5] Akihiro Harada[5] and Izamu Hatsukade[6]

[1]*Astrophysics Group, Cavendish Laboratory, Madingley Road, Cambridge CB3 0HE*
[2]*St John's College, Cambridge CB2 1TP*
[3]*Department of Physics, South Road, Durham DH1 3LE*
[4]*Department of Physics, Kyoto Sangyo University, Kamigamo-Motoyama, Kito-ku, Kyoto 603, Japan*
[5]*Department of Astrophysics, Faculty of Science, Nagoya University, Chikusa-ku, Nagoya 464-01, Japan*
[6]*Faculty of Engineering, Miyazaki University, 1-1 Gakuen-kibanadai-nishi, Miyazaki 889-21, Japan*

Accepted 2003 January 28. Received 2003 January 17; in original form 2001 March 20

ABSTRACT

We present new Ryle Telescope (RT) observations of the Sunyaev–Zel'dovich (SZ) decrement from the cluster Abell 773. The field contains a number of faint radio sources that required careful subtraction. We use *ASCA* observations to measure the gas temperature and a *ROSAT* HRI image to model the gas density distribution. Normalizing the gas distribution to fit the RT visibilities returns a value of H_0 of 77^{+19}_{-15} km s^{-1} Mpc^{-1} (1σ errors) for an Einstein–de Sitter universe, or 85^{+20}_{-17} km s^{-1} Mpc^{-1} for a flat model with $\Omega_\Lambda = 0.7$. The errors quoted include estimates of the effects of the principal errors: noise in the SZ measurement, gas temperature uncertainty and line-of-sight depth uncertainty.

Key words: galaxies: clusters: individual: A773 – cosmic microwave background – cosmology: observations – distance scale – X-rays: general.

1 INTRODUCTION

We have previously reported the detection of a Sunyaev–Zel'dovich (SZ) decrement (Sunyaev & Zel'dovich 1972) towards the $z = 0.217$ cluster Abell 773 using the Ryle Telescope (RT) (Grainge et al. 1993). [The SZ effect in this cluster has also been mapped by the millimetre array of the Owens Valley Radio Observatory (Carlstrom, Joy & Grego 1996a,b).] The RT observations of Abell 773 form part of a continuing programme to observe an X-ray luminosity-limited sample of rich, intermediate-redshift clusters in order to measure H_0 by combining SZ and X-ray observations (Jones et al. 2001). Such programmes (e.g. Mason, Myers & Readhead 2001; Reese et al. 2002; see also Birkinshaw 1999 for a review) are direct measurements of H_0 free from distance-ladder arguments.

In Grainge et al. (1993) we did not calculate an estimate of H_0 because no suitable X-ray image of A773 and no estimate of its gas temperature existed. A *ROSAT* HRI image and *ASCA* spectroscopic data have since become available, and we have also made additional RT observations. These now enable us to make an estimate of the Hubble constant from this cluster, which, when combined with other clusters from the sample, will give an estimate of H_0 unbiased by the individual shapes and orientations of the clusters.

⋆E-mail: kjbg1@mrao.cam.ac.uk
†Present address: Physics Department, Stanford University, CA 94305-4060, USA.

2 RYLE TELESCOPE OBSERVATIONS AND SOURCE SUBTRACTION

The RT (Jones 1991) is an east–west synthesis telescope of 13-m antennas with a bandwidth of 350 MHz and an average system temperature for these observations of 65 K at an observing frequency of 15.4 GHz. We used five antennas in a compact configuration, giving two baselines of 18 m, three of 36 m and five more out to 108 m. The short baselines alone are sensitive to the SZ signal; the longer ones are used to recognize and subtract the radio sources in the field that would otherwise mask the SZ decrement. We have made a total of 30 12-h observations of A773, each with the pointing centre RA$09^{\rm h}17^{\rm m}51\overset{\rm s}{.}91$, Dec. $+51^\circ43'32''$ (J2000). Phase calibration using 0859+470 and flux calibration using 3C 48 and 3C 286 were carried at as described in Grainge et al. (1993). Similarly, we used the POSTMORTEM package (Titterington 1991) to flag the data for interference and antenna pointing errors, and to weight them in accord with the continuously monitored system temperature of each

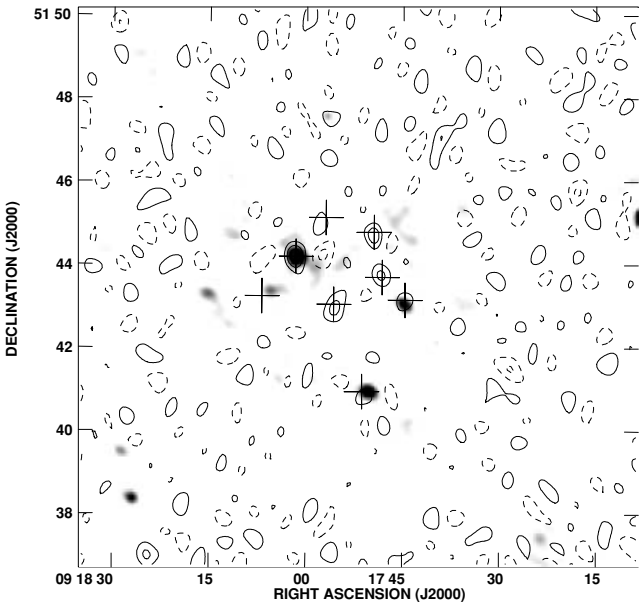

Figure 1. Map of the longer baseline RT data (2 kλ upwards) (contours) plus a VLA 1.4-GHz observation (grey-scale), jointly used to determine initial source positions for the source subtraction procedure. The crosses show the positions of the subtracted sources listed in Table 1. The contour interval is 70 μJY, dashed contours are negative; the grey-scale runs from 0.3 (light) to 1.0 mJy (dark). The RT data have not been corrected for the effect of the telescope primary beam (FWHM = 6 arcmin).

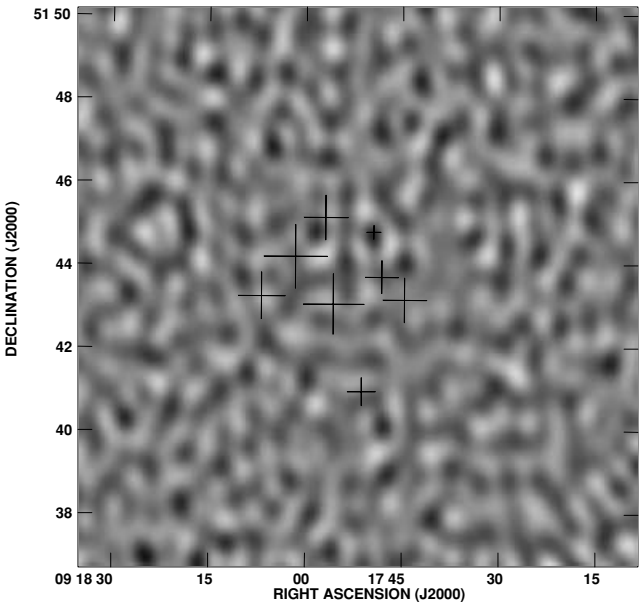

Figure 2. Map of the longer baseline data (2 kλ upwards) after source subtraction, showing no significant residual features. The crosses show the positions of the subtracted sources listed in Table 1; the size of the cross is proportional to the flux subtracted. The grey-scale runs from −200 (light) to 200 μJY (dark). The data have not been corrected for the effect of the telescope primary beam.

antenna. As a standard check, we used the AIPS package to make a map of each 12-h run and then combined the data.

We removed radio sources from the data by a simultaneous maximum-likelihood fit to several point sources and the SZ effect using a technique described by Grainger et al. (2002). We use a model for the SZ signal as a function of the baseline that is based on the β-model fit to the X-ray image described below (Section 3). We simultaneously fit flux densities for trial sources, the initial positions of which are determined both from a map made from just the long-baseline data (>2 k λ), and from a VLA 1.4-GHz image of the cluster field (Fig. 1). This allows us to fit the optimum flux densities of sources, the existence of which we know of from the VLA image but that would not give a significant detection from the RT data alone. The positions and fitted flux densities are given in Table 1. The image made from the long (>2 k λ) source-subtracted baselines is consistent with noise (Fig. 2).

Table 1. Flux densities and positions of sources removed from the A773 field. Flux densities are apparent, i.e. not corrected for the RT primary beam response, and are all ±35 μJY. Offsets are relative to the pointing centre of $09^{\rm h}17^{\rm m}51\overset{\rm s}{.}91 + 51^\circ43'\,32''$(J2000).

Flux density (μJy)	RA offset (arcsec)	Dec. offset (arcsec)
163	−67	−23
123	−34	9
55	−22	75
103	−5	−155
228	35	−29
162	46	96
238	90	40
177	139	−16

To image the decrement, we removed the sources in Table 1 from all the visibilities and made a short-baseline map from baselines shorter than 1 kλ, and CLEANed this. The resulting image is shown in Fig. 3. The decrement is of −527 μJy beam^{-1} with a noise (1σ) of 60 μJy beam^{-1}; the beam is 152 × 119 arcsec^2 FWHM. Also shown is the X-ray image of the cluster; it can be seen that the alignment

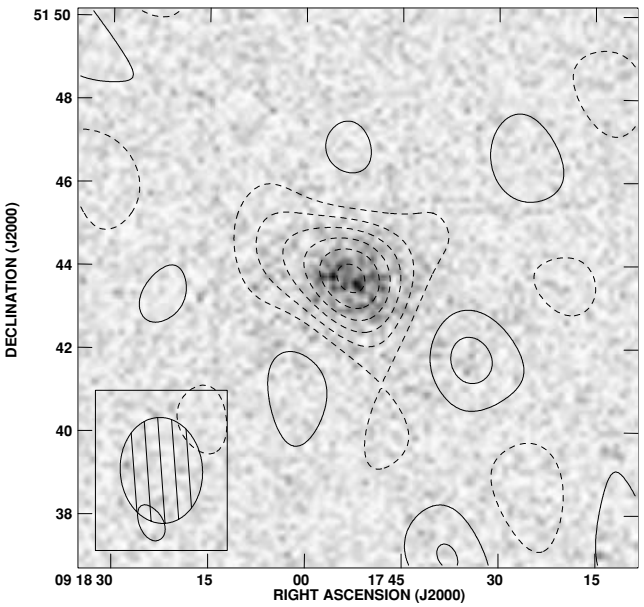

Figure 3. X-ray and SZ images of A773. The grey-scale is the *ROSAT* HRI image; contours are the source-subtracted and CLEANed RT image. Contours are in multiples of 80 μJY beam^{-1}, dashed contours are negative. The restoring beam (shown) is 152 × 119 arcsec^2, PA = 4° and the data have not been corrected for the effect of the telescope primary beam.

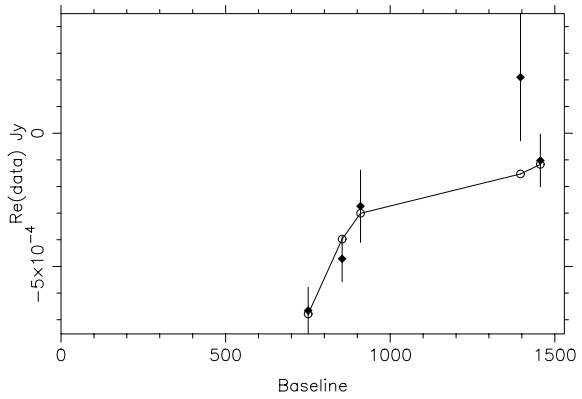

Figure 4. The real part of the source-subtracted visibilities as a function of baseline in wavelengths (filled points with error bars), with the best-fitting SZ model (open points joined by lines).

with the X-ray image is very good. The extension of the SZ image to the northeast is of marginal significance. The magnitude of the decrement is consistent with that of -590 ± 116 μJY, in the same beam, reported in Grainge et al. (1993).

An alternative way of looking at the data is shown in Fig. 4, which shows the real part of the source-subtracted visibilities binned radially, along with the best-fitting model based on the X-ray data. These data have the advantage, unlike the image pixels, of having independent Gaussian noise on each point; it is these that are used in fitting for H_0.

3 X-RAY OBSERVATIONS AND FITTING

We measure the gas temperature from *ASCA* observations on 1994 April 29 of 46 240 s (GIS) and 39 904 s (SIS), using standard XSPEC tools. Times of high background flux were excluded and both GIS and SIS data were used. We took the Galactic absorbing column density predicted by Dickey & Lockman (1990) in the direction of A773 of 1.3×10^{24} H atom m^{-2}. Using a Raymond–Smith model, we find a temperature of 8.7 ± 0.7 keV (90 per cent confidence error bounds) and a metallicity of 0.25 solar. The 2–10 keV flux from A773 is $6.7 \pm 1.0 \times 10^{-13}$ W m^{-2}. Our temperature estimate is consistent with that of Allen & Fabian (1998) who find a temperature of $9.29^{+0.69}_{-0.60}$ keV (90 per cent confidence error bounds).

For the X-ray surface-brightness fitting we used a *ROSAT* HRI image of A773 with an effective exposure of 16 518 s obtained on 1994 April 13–15 and analysed using standard ASTERIX routines. We calculate the *ROSAT* HRI count rate, given our estimates of metallicity and Galactic column and with the K-correction appropriate to the redshift of A773, to be 1.53 ($\pm$0.08) $\times 10^{-69}$ count s^{-1} from a 1 m^3 cube of gas of electron density 1 m^{-3} at the temperature of A773 and at a luminosity distance of 1 Mpc.

We then fitted an ellipsoidal King profile to the X-ray image. Since the high spatial resolution of the HRI leads to a low count rate per pixel, we use Poisson rather than Gaussian statistics to fit for the measured count in each pixel. For c_i counts measured at position x_i, and for a mean number of counts $f(x_i \mid a)$ predicted by the model given parameters a (such as core radius), the probability of obtaining c_i counts is

$$P(c_i \mid a) = \frac{[f(x_i \mid a)]^{c_i}}{c_i!} \mathrm{e}^{-f(x_i \mid a)},$$

and the most probable value of a can be obtained in a computationally efficient way by maximizing

$$\ln P(c \mid a) = \sum_i [c_i \ln f(x_i \mid a) - \ln c_i! - f(x_i \mid a)].$$

We fitted an ellipsoidal King profile to the HRI data with θ_1 and θ_2 as the perpendicular angular sizes in the plane of the image, assuming that the length along the line of sight is the geometric mean of the other two. We find $\theta_1 = 60$ arcsec and $\theta_2 = 44$ arcsec, with the major axis at position angle 16°, $\beta = 0.64$, and central electron density $n_0 = 6.80 \times 10^3\, h_{50}^{-1/2}$ m^{-3}, where $H_0 = 50\, h_{50}$ km s^{-1} Mpc^{-1}. Fig. 5 shows the HRI image, the model, and the residual image with the best model subtracted. To assess the goodness of fit, we made 50 realizations of the image with the appropriate Poisson noise added, and calculated the mean and standard deviation of their Poisson likelihoods. The likelihood of the observed HRI image is 0.32 standard deviations from the mean; we therefore conclude that the fit is good and the cluster is well represented by a β model.

There is a strong degeneracy in the fit between β and $\theta_{1,2}$; however, this has little effect on the comparison with the SZ data and the derived value of H_0. Fig. 6 shows the likelihood contours for the fit in the β–θ_1 plane, marginalized over n_0 and using the best-fitting value of the axial ratio (which is very well constrained). Overlaid are the contours of the predicted mean observed SZ flux density on the shortest RT baseline. It can be seen that despite the degeneracy between β and θ_1, the range of SZ flux densities corresponding to the 1σ limits of the model fit is only $\pm$3 per cent. Since the SZ flux density varies as H_0^{-2}, this corresponds to a 6 per cent error in H_0 owing to the model fitting. This lack of sensitivity to the β–θ degeneracy is characteristic of observations that are sensitive to spatial frequencies around the cluster core size (see, e.g., Reese

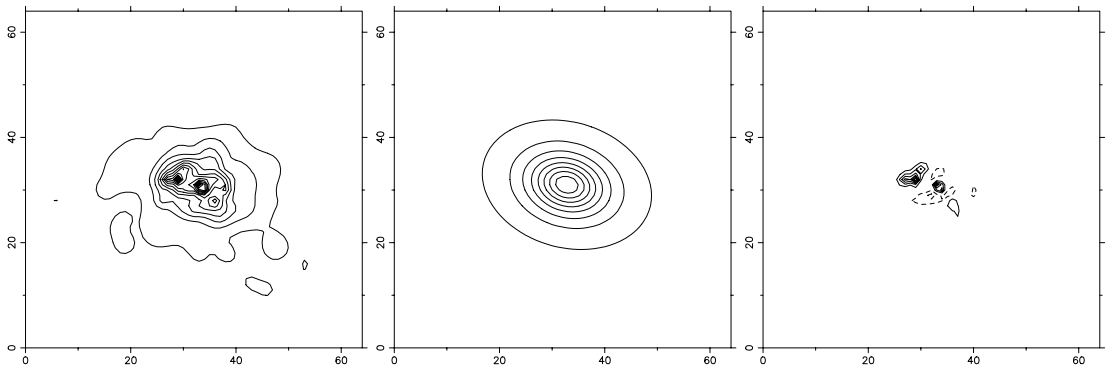

Figure 5. X-ray model fits. Left: *ROSAT* HRI image of A773; centre: the best-fitting model X-ray surface brightness; right: The difference between the data and the model, which is consistent with the Poisson noise in the data. The contour interval is 1 count per 8-arcsec pixel.

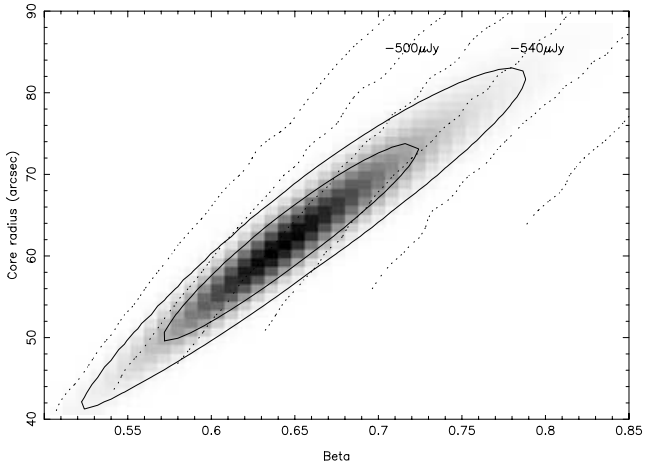

Figure 6. Solid contours and grey-scale: the likelihood of the fitted X-ray model as a function of β and θ_1, marginalized over n_0, with the axial ratio and position angle fixed at their most probable values. The solid contours enclose 67 and 95 per cent of the likelihood. Overlaid are dotted contours of the predicted mean flux on the shortest RT baseline for the given model parameters (using the most probable value of n_0); the contour interval is 40 μJy. Since the normalization of the SZ flux relative to the X-ray is what controls the fit for h, this figure shows the insensitivity of our H_0 determination to the degeneracy in the X-ray model fit.

et al. 2000) and contrasts with the sensitivity to the model fitting of measurements that measure only lower spatial frequencies (e.g. Birkinshaw & Hughes 1994).

4 H_0 ESTIMATION

To measure H_0, we compared the real SZ data with a simulation of the SZ effect from the X-ray gas model. We use the expression of Challinor & Lasenby (1998) to provide a relativistic correction to the standard non-relativistic SZ expression; in the case of A773, the effect is to increase our estimate of the y-parameter by 2.4 per cent. We then simulated RT observations of the SZ effect owing to the model gas distribution and compared these with the real source-subtracted RT visibilities on the same baselines, and adjusted H_0 to obtain the best fit. Using our temperature of 8.7 ± 0.7 keV we find $H_0 = 77^{+13}_{-11}$ km s^{-1} Mpc^{-1}, assuming an Einstein–de Sitter universe. The 1σ error quoted is that due solely to noise in the SZ data. For the best-fitting β, $\theta_{1,2}$ model, the corresponding central density n_0 is 8.44×10^3 m^{-3} and the central decrement is 737 ± 85 μK.

Grainge et al. (2002) consider at some length the contributions to the error in the H_0 determination from A1413. The situation in A773 is very similar. The dominant contributions to the error in H_0 in A773 are ±16 per cent from noise in the SZ measurement, ±12 per cent from our estimation of the gas temperature and a probable error of ±14 per cent from the uncertain line-of-sight depth.

Table 2. Error budget for the H_0 calculation; the dominant terms are the errors in the SZ measurement and the gas temperature. The errors are all multiplicative, i.e. the 1σ limits on H_0 are $77 \times 1.25 = 96$ and $77/1.25 = 62$ km s^{-1} Mpc^{-1}.

Source of error	Error contribution to H_0
SZ measurement	±16 per cent
Line-of-sight depth	±14 per cent
Gas temperature	±12 per cent
Error in calculated X-ray emission constant	±6 per cent
Primary flux calibration	±2.5 per cent
Total (in quadrature)	±25 per cent

This is obtained by considering the range of axial ratios of simulated clusters that is needed to reproduce the projected axial ratio distribution observed in clusters with redshift similar to that of A773 (Grainger 2001). Clearly, this estimate is rather uncertain for a single object, but can be significantly reduced by averaging a sample of clusters with random orientations. Table 2 shows the complete error budget, and the final 1σ error limits of $H_0 = 77^{+19}_{-15}$ km s^{-1} Mpc^{-1} if $(\Omega_m, \Omega_\Lambda) = (1.0, 0.0)$ and $H_0 = 85^{+20}_{-17}$ km s^{-1} Mpc^{-1} if $(\Omega_m, \Omega_\Lambda) = (0.3, 0.7)$.

5 CONCLUSIONS

Using *ASCA*, *ROSAT* HRI and RT observations of A773, we find:

(i) there are eight radio sources detectable in the field of the cluster that we have removed from the data, which would otherwise contaminate the measurement of the SZ effect;

(ii) the correlated fitting errors on the shape parameters β and θ have a negligible effect on the derived value of H_0, a feature characteristic of observations on the scale of the cluster core size;

(iii) the estimated value of H_0 is 77^{+19}_{-15} km s^{-1} Mpc^{-1} if $(\Omega_m, \Omega_\Lambda) = (1.0, 0.0)$ or 85^{+20}_{-17} km s^{-1} Mpc^{-1} if $(\Omega_m, \Omega_\Lambda) = (0.3, 0.7)$, where the 1σ error bars include estimates from the main sources of error – noise in the SZ data, X-ray temperature uncertainty and uncertain line-of-sight depth.

ACKNOWLEDGMENTS

We thank the staff of the Cavendish Astrophysics group who maintain and operate the Ryle Telescope, which is funded by PPARC. AE acknowledges support from the Royal Society; WFG acknowledges the support of a PPARC studentship; RK acknowledges support from an EU Marie Curie Fellowship.

REFERENCES

Allen S.W., Fabian A.C., 1998, MNRAS, 297, L57
Birkinshaw M., 1999, Phys. Rep., 310, 97
Birkinshaw M., Hughes J.P., 1994, ApJ, 420, 33
Carlstrom J.E., Joy M., Grego L., 1996a, ApJ, 456, L75
Carlstrom J.E., Joy M., Grego L., 1996b, ApJ, 461, L59
Challinor A., Lasenby A., 1998, ApJ, 499, 1
Dickey J.M., Lockman F.J., 1990, ARA&A, 28, 215
Grainge K., Jones M., Pooley G.G., Saunders R., Edge A.C., 1993, MNRAS, 265, L57
Grainge K., Jones M.E., Pooley G.G., Saunders R., Edge A.C., Kneissl R., 2002, MNRAS, 333, 318
Grainger W.F., 2001, PhD thesis, Univ. Cambridge
Grainger W.F., Das R., Grainge K., Jones M.E., Kneissl R., Pooley G.G., Saunders R., 2002, MNRAS, 337, 1207
Jones M.E., 1991, in Cornwell T.J., Perley R., eds, Proc. IAU Colloq. 131, ASP Conf. Ser. 19, Radio Interferometry: Theory, Techniques and Applications. Astron. Soc. Pac., San Francisco, p. 395
Jones M.E. et al., 2001, MNRAS, submitted
Mason B.S., Myers S.T., Readhead A.C.S., 2001, ApJ, 555, L11
Reese E.D. et al., 2000, ApJ, 533, 38
Reese E.D., Carlstrom J.E., Joy M., Mohr J.J., Grego L., Holzapfel W.L., 2002, ApJ, 581, 53
Sunyaev R.A., Zel'dovich Ya B., 1972, Comm. Astrophys. Space Phys., 4, 173
Titterington D.J., 1991, in Cornwell T.J., Perley R., eds, Proc. IAU Colloq. 131, ASP Conf. Ser. 19, Radio Interferometry: Theory, Techniques and Applications. Astron. Soc. Pac., San Francisco, p. 128

This paper has been typeset from a TEX/LATEX file prepared by the author.